

# Automatic counting of FISH spots in interphase cells for prenatal characterization of aneuploidies

Ilya Ravkin\* and Vladimir Temov  
 Applied Imaging Corp., Santa Clara, CA 95051

## ABSTRACT

Fluorescent In-Situ Hybridization (FISH) is becoming an accepted technique for identification of aneuploidies in interphase fetal cells obtained by either CVS (chorionic villus sampling) or amniocentesis. Currently the analysis is done manually by a skilled operator and is a lengthy and fatiguing process. Applied Imaging is developing an automated procedure for counting FISH spots in these samples. Spot counting involves slide preparation, probe hybridization, filter selection, FISH image acquisition, image analysis, operator verification, and analysis of count distributions.

We concentrate on the tasks starting with image acquisition. The following topics are covered: selection of appropriate cells, acquisition and processing of Z-stacks of FISH images for presentation and spot counting, background removal, formation of segmentation tree and selection of spot markers, growing of spot markers by means of constrained watershed, detection of irregular spots and flagging them for the user, time and accuracy compared with manual method, and applicability to a clinical research setting.

**Keywords:** image cytometry, automated microscopy, DNA probes, FISH

## 1. SAMPLES AND SLIDE PREPARATION

The use of FISH for the rapid diagnosis of prenatal numerical chromosomal abnormalities is of importance in critical cases when limited time is left for the option of the terminating the pregnancy<sup>1,2</sup>. It is also of importance in the reduction of maternal anxiety since results can be obtained in hours as opposed to days or weeks using traditional karyotyping. Nevertheless, the widespread use of FISH in prenatal diagnosis has been hindered by the difficulties encountered when applying interphase FISH to uncultured amniotic fluid cells (amniocytes). Because of the high numbers of dead and morphologically aberrant cells, analysis of FISH on amniocytes is especially onerous and time-consuming (Fig 2). The availability of an instrument that could automatically reject unreadable cells and collect data only on the informative ones would be of great value in the clinical laboratory.

X probe	Composite with nucleus	Counts by 8 operators, (* reject)	X probe	Composite with nucleus	Counts by 8 operators, (* reject)	X probe	Composite with nucleus	Counts by 8 operators, (* reject)
		2, *, 3, 2, 3, 2, *, 3			2, 2, 3, 2, 3, 1, 2, 1			2, 4, 2, *, 2, 3, *, 3
		3, 3, 4, 4, 3, 3, *, 3			2, 2, 3, 1, 3, 2, 2, 2			1, 1, 2, *, 1, 2, *, 1
		2, 2, 3, *, 3, 2, *, 3			3, 4, 3, 3, 3, 2, 4, 3			1, 1, 2, 2, 1, 2, 2, 1

Fig. 1. Ambiguous cells and manual counts.

Examples of cells from a Vysis ProbeCheck control slide with cultured normal lymphocytes probed for X and Y chromosomes and counted from the screen images by 8 skilled operators.

\* Correspondence: Email: [iravkin@compuserve.com](mailto:iravkin@compuserve.com); Telephone: 408-450-4335.

Amniotic samples were obtained from pregnant women between 13 and 33 weeks of gestation (average 16 weeks). Approximately 5 ml of amniotic fluid was used to prepare the slides. Briefly, uncultured amniocytes were washed and resuspended in 0.1 ml of PBS. Next, 0.025 ml of cell suspension was placed at two positions on cleaned glass slides and treated according to the method provided by the DNA probe vendor. One position was probed for chromosomes X,Y and 18, and the other position for chromosomes 13 and 21. Chromosome specific probes were obtained commercially (Vysis Inc., Downers Grove, IL) and Fluorescent In-Situ Hybridization and manual spot counting was done according to vendors instructions.

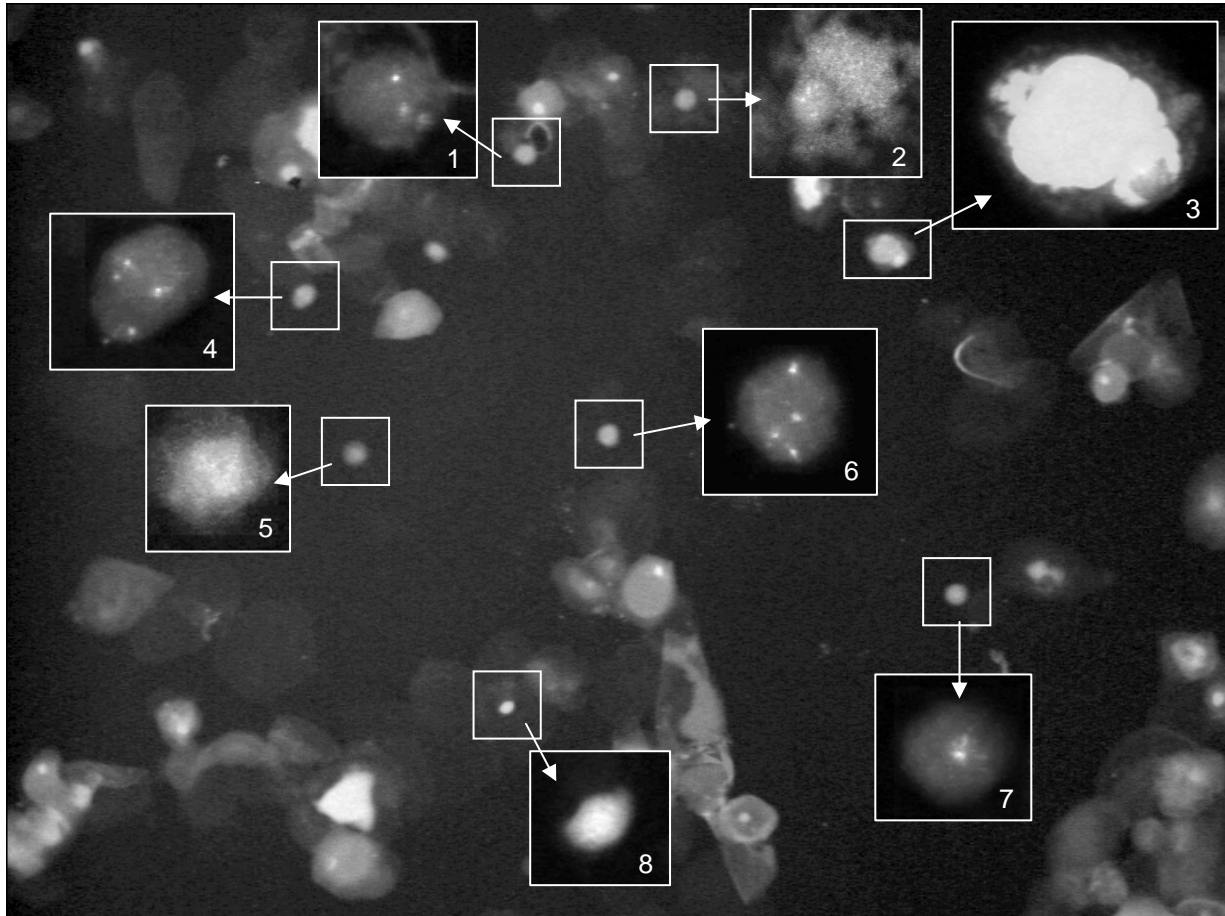


Fig. 2. A typical microscope field of view on a slide containing amniotic fluid cells. The whole field was acquired with a 10X objective using a Vysis quad filter set: DAPI, Aqua, SpectrumGreen, and SpectrumOrange. The multicolor image was then converted to grayscale for reproduction. The inserts were acquired with a 40X objective using the SpectrumGreen filter for chromosome 13 and the SpectrumOrange filter for chromosome 21. This field illustrates some of the problems found in the FISH analysis of slides containing amniotic fluid cells. Images 1,4,6, and 7 show cells with defined nuclear morphology and clear chromosomal fluorescent signals. Images 2,3,5 and 8 show cells with amorphous nuclei, high autofluorescence and no chromosome signals.

Before proceeding with the development of automated spot counting we tested the consistency of manual spot counting and clarity of the counting instructions supplied with the probes. We used Vysis ProbeCheck control slide with cultured normal lymphocytes probed for X and Y chromosomes. An area of a slide was scanned and 1100 images for manual counting were acquired at 20X objective magnification. From this number 55 cell images were selected and presented to eight operators skilled in the art. Of those cells 43 received different counts, sometimes with a discrepancy of 2 spots. Selected cells are shown in Fig. 1. Uncultured amniocytes are much more difficult to analyze than cultured lymphocytes, therefore as many as half of the cells with apparently non-damaged nuclei cause disagreements in the counting. As a result, no attempt was made to interpret difficult cases as split or merged spots<sup>4</sup>. Instead, rules were defined to separate ambiguous from unambiguous cells.

This work is based on the automated microscopy system described previously<sup>3</sup>.

## 2. SELECTION OF CELLS FOR SPOT COUNTING

The strategy for selection of cells for spot counting is determined by the balance of time required for the different ways of assessing cell acceptability. The feature that is most easily determined is the DAPI stained cell nucleus. The first scenario is scanning for nuclei with 10X objective and selection of a certain number of cells by nuclear size, shape and intensity (Fig. 3). Speed of scan is 6 to 12 min./cm<sup>2</sup> depending on DAPI brightness and cell density.

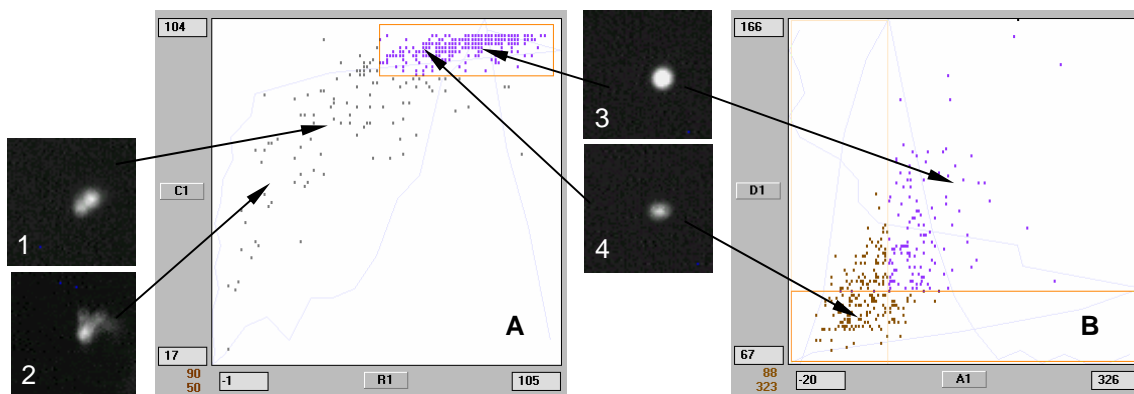


Fig. 3. Selection of best nuclei after scanning.

A - distribution of nuclei by compactness (Y axis) and roundness (X axis). Outlined rectangle contains nuclei that are visually not damaged.

B - after the shape selection the nuclei are selected by area (X axis) and density (Y axis).

1 - two touching nuclei, 2 - damaged nucleus, 3,4 - round nuclei of different size and brightness.

Next, the 40X images are acquired for spot counting (see below). Nuclear appearance is not a very good predictor and more than half of the cells are still unusable for spot counting, mostly due to high autofluorescence (e.g.: cells 2, 5, 8 in Fig. 2).

The second scenario is to scan with a 20X objective for the presence of at least one probe signal within the nuclear boundary. Although this magnification is not sufficient for accurate spot counting, it is suitable for eliminating autofluorescing cells and cells with no probe signals (Fig 4).

Fig. 4. Scan for cells containing probe spots.

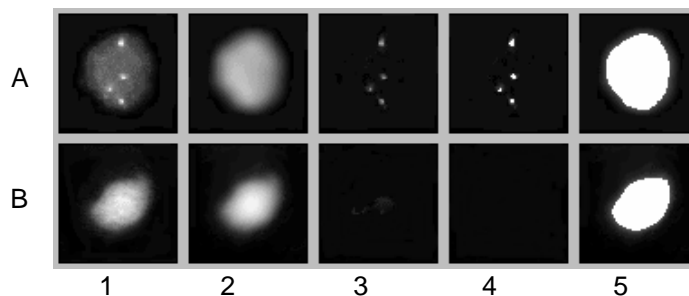
A - cell #6 from Fig. 2 contains probe spots,

B - cell #8 from Fig. 2 is an artifact.

1 - probe image, 2 - DAPI image,

3 - probe spots after background removal,

4 - detected spots, 5 - nuclear mask.



The scan is performed with two filters, one for DAPI, another for the probe that is most likely to have artifacts. Autofocusing is done on DAPI,

other details are described previously<sup>3</sup>. This latter type of scan is much slower, but practically every cell selected is usable for counting. Scan speed is 30 to 80 min./cm<sup>2</sup> depending on the probe and DAPI brightness and cell density. The decision on which strategy to use depends on the nature of the slide.

## 3. ACQUISITION OF FISH IMAGES

Preliminary investigation found that a 40X objective (0.75 NA) gives adequate results for manual counting of FISH signals on the microscope or from the computer screen. Importantly, it was also found that during inspection under the microscope, operators routinely vary focus on almost every cell to see probe spots in their best focal position. In order to match quality of spot counting from the screen to that from the microscope, all images presented for counting were produced as a maximum projection of the Z-stack. Thickness of specimens used in this study is 2-3  $\mu$ m. Depth of field with the 40X objective is about

1  $\mu\text{m}$ . Probe spots that differ in the Z plane but are at the same XY position in the cell are probably unresolvable. The purpose of Z-stack is not to resolve spots in Z dimension, but to create a single image in which each spot is represented as if it were in the best focus. This is especially important for spots acquired with different filters, since the difference in focal position can also be due to chromatic aberrations.

Maximum projection is the simplest method of combining planes in Z-stack, but whether it is adequate in our case is questionable. We compared this method to maximum projection after deconvolution by constrained iterative algorithm from the MicroTome package (VayTek, Inc., Fairfield, IA). An example is in Fig. 5. The deconvolved images are cleaner, but for the purpose of spot counting there is no useful difference.

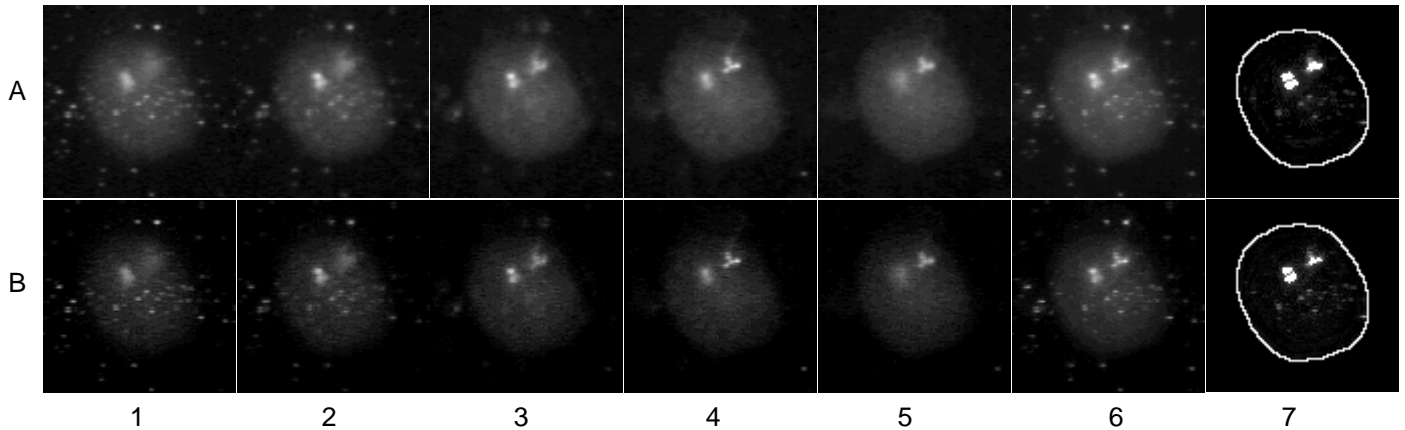


Fig. 5. Processing of Z-stack.  
 A1-A5 - a stack of images of chromosome 18 (Vysis SpectrumAqua) acquired with an Olympus UPlanFI 40X/0.75 objective. The separation between planes is 0.8  $\mu\text{m}$ . A6 - maximum projection of A1-A5. A7 - spots, detected in A6, superimposed on the probe image within nuclear outline.  
 B1-B5 - deconvolution of stack A1-A5 using constrained iterative algorithm with theoretical point spread function, courtesy of VayTek, Inc. (Fairfield, IA), B6 - maximum projection of B1-B5. B7 - spots, detected in B6, superimposed on the probe image within nuclear outline.

Z-stack is also necessary because after relocating to a cell, focusing must be done on the DAPI image. Probe spots are too small and too dim to allow focusing from a large offset. The best focus position for DAPI may not be the best focus position for any of the probes. Besides, the focusing curve for DAPI is not very sharp, so the autofocus position is not very precise. The probe acquisition procedure is illustrated in Fig. 6. Typically, the time required for this procedure on one cell is 20 to 30 seconds.

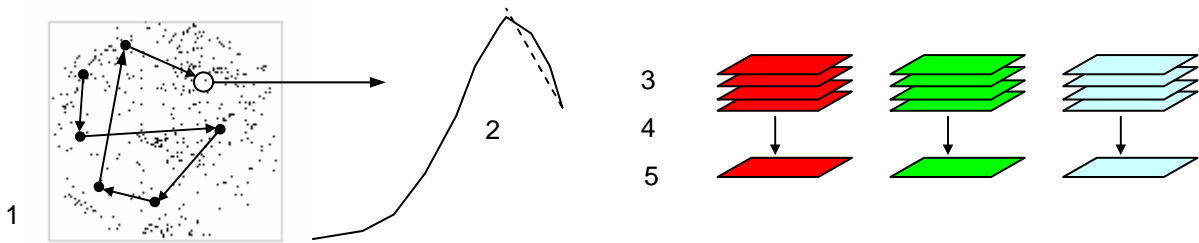


Fig. 6. FISH acquisition procedure.  
 1. Relocate to a cell from the list of cells selected in the previous section.  
 2. Autofocus on the nuclear counterstain.  
 3. For each probe, acquire a Z stack with a small number of planes (5-8), separated by 0.5-0.8  $\mu\text{m}$  (for 40X objective).  
 4. For each plane, remove the low frequency background, usually just the constant level.  
 5. Combine all planes in the stack by maximum projection.

## 4. COUNTING OF PROBE SPOTS

Counting of probe spots in interphase nuclei has received some attention lately<sup>4,5,6,7</sup>. The difference in our approach is the separation of cells into two classes: cells with unambiguous spots and cells with ambiguous spots. The goal is to find a subpopulation of cells on which the counts are the same among different operators and the machine. This requires accurate outlining of spots in order to flag them by size, shape, intensity, etc. The outlining of spots must be visually correct. The disagreement between operators is not that they see the blips of brightness differently, rather that they interpret them differently as probe hybridization sites (probe signals). We attempted to identify the peaks of brightness as close to how a human does it but leave all the interpretation to him except for the unambiguous cases.

Counting of spots is done independently for each probe but the overlapping of spots in different filters is flagged. This may be caused by fluorescing debris. It is assumed that the nucleus of the cell is known, typically from a separate image of nuclear counterstain, or that it can be extracted from the probe image.

### 1. Preprocessing

Preprocessing is essentially the same as in Netten et al.<sup>4</sup> Opening<sup>8</sup> of the original image with an appropriate size structuring element is subtracted from the original. The size of the structuring element is a parameter of the algorithm and is scaled by magnification.

### 2. Formation of segmentation tree and selection of markers

The segmentation tree starts to grow up from the marker threshold  $T_M$  which is set high enough to exclude undesired areas but low enough to include at least a few pixels of all potential spots. For each connected set, the threshold is raised independently until the set splits into several new sets or disappears. If a new set has an area smaller than  $AM_{Min}$  it is not considered a potential marker and its branch of the tree is stopped (Fig. 7,  $M_3$ ).  $AM_{Min}$  controls the size of the detail of the brightness distribution, which is considered “noise”. In order for this area to be considered as part of another spot, the relief is razed to the level before the split. At the end of the procedure, leaves of the tree are spot markers. To speed up the growing of spots, the actual markers are made by a section of the tree, which gives them maximal area without merging and not exceeding  $AM_{Max}$ . If a marker is bigger than the maximal area allowed for a spot  $AS_{Max}$ , then the marker is rejected (Fig. 7,  $M_4$ ). This is the case of big saturated spots.

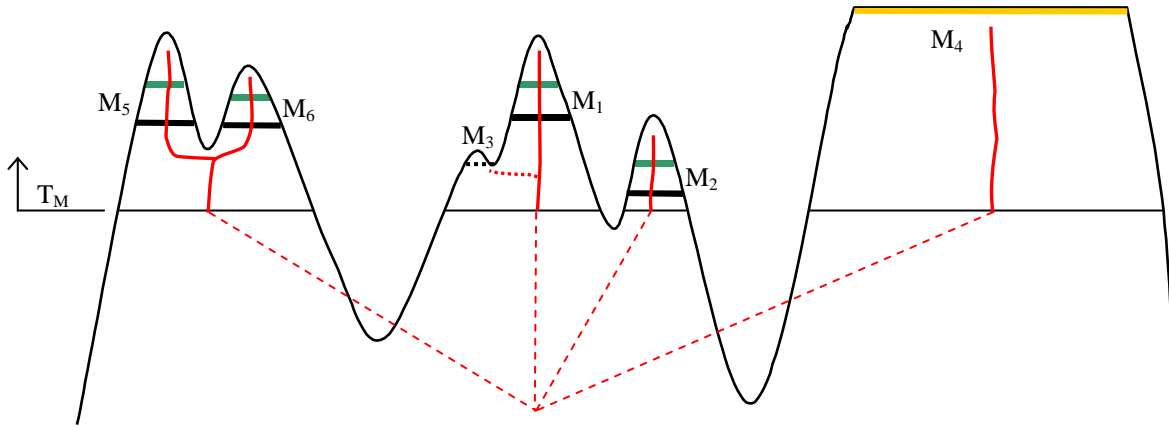


Fig. 7. Formation of spot markers.

$T_M$  - marker threshold from which the segmentation tree starts growing up.

$M_5$ ,  $M_6$ ,  $M_1$ ,  $M_2$  - accepted markers. For each marker the higher line is the smallest set before it disappears or becomes smaller than minimum for a marker, the lower line is the representation of the marker used for spot growth.

$M_3$  - marker rejected because after splitting it has area smaller than minimum for a marker.

$M_4$  - marker rejected because it has area larger than maximum for a spot.

### 3. Growth of spot markers



Briefly, spots grow in a queue, which is sorted by spot threshold (defined as lowest pixel in the spot). The spot at the top of the queue is attempted to grow by adjoining the most appropriate pixel. If this occurs, the queue is resorted and the process repeats till there are no more pixels that could be added without violating one of the conditions. The following pseudocode describes the algorithm in more detail and Fig. 8 gives its graphical representation:

```

Repeat while there are spots in the queue.
    If area of the current spot  $\geq AS_{Max}$ , then the spot is ready, delete it from the queue, and continue the main loop.

    Form the contour of the current spot.
    Exclude from the contour all pixels below spot threshold  $T_S$ .
    Exclude from the contour all pixels, which are neighbors of any other spot (non-merge condition).
    Exclude from the contour all pixels that are higher than all their neighbors belonging to the spot (watershed condition)

    If the contour is empty, then the spot is ready, delete it from the queue, and continue the main loop.

    Find the maximal pixel in the remainder of the contour.
    Calculate form factor after adjoining this pixel (see Fig 9).

    If form factor  $< F_{Min}$ , then the spot is ready, delete it from the queue, and continue the main loop.

    Resort spot list (after adding the pixel, the spot threshold may have changed).
End
    
```

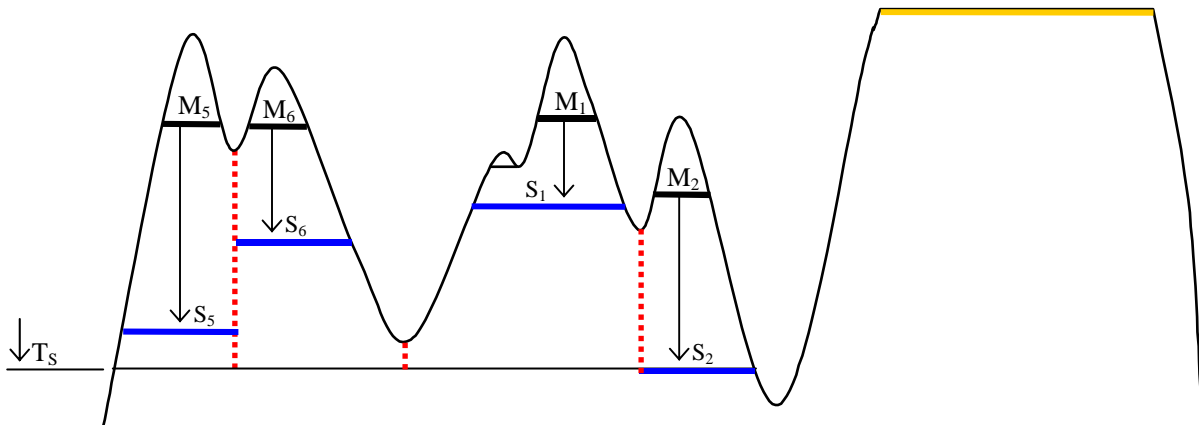
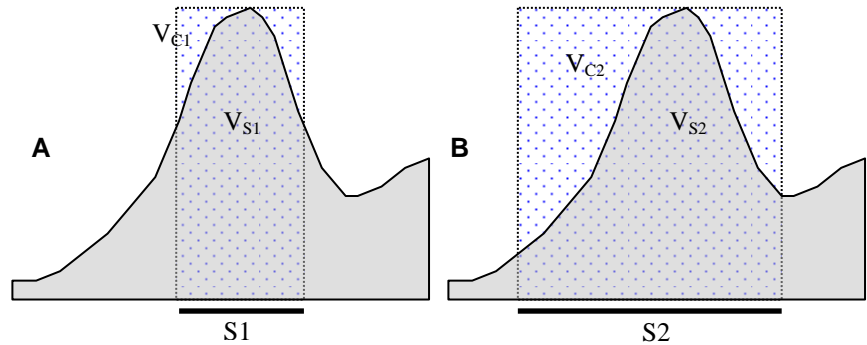


Fig. 8. Spot growth. Growth of a spot starts with a previously found marker and is restricted by the watershed<sup>9</sup> dividers (dotted vertical lines) of the relief, by spot threshold ( $T_S$ ), by maximal spot area ( $AS_{Max}$ ), and by minimal form factor ( $F_{Min}$ ).

Fig. 9. Form factor.  
 $F = V_S/V_C * 100$ , where  $F$  is the form factor,  $V_S$  is the spot volume,  $V_C$  is the volume of the cylinder with the same base as the spot and height equal to the spot maximum.  
 A and B are two iterations of spot growth. As the spot grows the form factor decreases. When it reaches a predefined limit  $F_{Min}$  the growth stops. The form factor defined here is sensitive to the brightness histogram in the spot, but not to its shape. Other functions decreasing with spot growth could be used as well.



#### 4. Flagging of suspicious cells

After the spots in the nucleus are determined and analyzed, if they do not meet the set of conditions defined below, the cell is flagged as needing operator review (Fig. 10). For each spot a set of parameters is calculated and compared to the predefined limits. In addition, for some parameters average values for all spots in the cell are calculated and spot parameters are compared to the cell average.


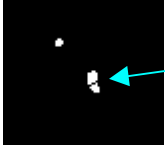

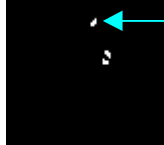

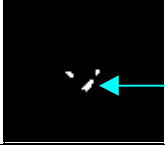
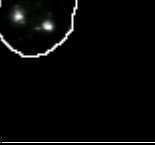


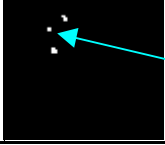

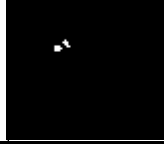
Spots with superimposed nuclear contour	Result of spot detection	Reason for flagging	Spots with superimposed nuclear contour	Result of spot detection	Reason for flagging
		separation			average over threshold, nonuniform interspot distance
		roundness, compactness, average over threshold			nucleus not completely in the image
		area, average over threshold			nucleus not round

Fig. 10. Examples of flagged cells.


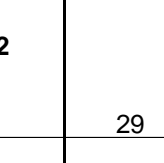
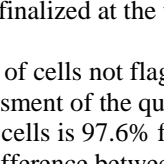
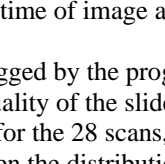
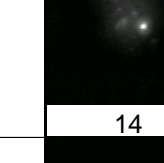
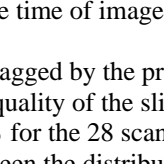
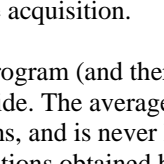
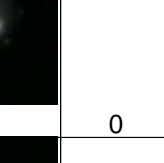
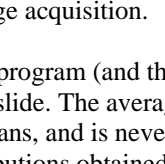
Acceptance conditions:

1. Area of a spot must be between  $AS_{Min}$  and  $AS_{Max}$ .
2. Average pixel value of a spot must be  $\geq P_{Min}$ .
3. Average pixel value above spot threshold must be  $\geq PT_{Min}$ .
4. Compactness of a spot must be  $\geq C_{Min}$ . Compactness is defined as the ratio of the central moment of inertia<sup>10</sup> of a disk with the same area as of the given shape to the central moment of inertia of the shape itself. This ratio does not exceed 1 and is normalized to the range 0 - 100. Small values are typical for ring-like, star-like or irregular shapes, large values are typical for compact (and round) objects.
5. Roundness of a spot must be  $\geq R_{Min}$ . Roundness is defined as the ratio of the shortest main inertia axis<sup>10</sup> to the longest one, normalized to the range 0 - 100. Small values are typical for elongated shapes, 100 is for circular objects.
6. Convexity of a spot must be  $\geq V_{Min}$ . Convexity is defined as the ratio of the spot area to the area of its minimal enclosing convex shape. As an approximation for the convex shape we use the 16-sided polygon. This ratio does not exceed 1 and is normalized to the range 0 - 100.
7. Separation between a spot and its neighbors must be  $\geq Sep_{Min}$ . This parameters can be calculated if there are more than one spot. It is defined as the ratio of squared distance between two spots to the sum of their areas. This ratio is multiplied by 100. The distance between spots is defined as the distance between maximal pixels in each spot.
8. If there are more than one spot, then averages are calculated for area, average pixel value, and distance to the nearest neighbor. If the difference between any of the above parameters and their average in the cell divided by this average is greater than maximal allowed deviation  $Dev_{Max}$ , then the cell is flagged. Such condition often indicates split, merged or otherwise unusual spots.
9. The nuclear mask is also subjected to several tests. The area must be within given limits. Compactness and roundness must be equal or higher than given minima. These conditions reject damaged and touching nuclei (that were not rejected at lower magnification). Also the nuclear mask must be completely within the acquired image, if it touches the boundary, the cell is flagged.

## 5. RESULTS

Data was collected as follows. In each slide an area of 30 to 100 mm<sup>2</sup> was scanned for DAPI stained nuclei at magnification 10X. The 100 to 150 best nuclei, as determined by shape and intensity, were selected for probe acquisition at 40X. Next, the cells with damaged nuclei or high autofluorescence were further rejected. The remaining cells were scored by the operator and by the program. Program spot counts were done with the same values of parameters for all samples. Fig. 11 shows typical examples of spots and their manual and program counts on a CVS sample with trisomy 21.

Fig. 11. Results of manual and program spot counting on a CVS sample with trisomy 21. Images are typical examples in their categories. All not flagged cells were counted correctly. Spot distribution by manual count and by not flagged program count has no significant difference ( $\chi^2=0.27$ ,  $df=3$ ,  $p=0.966$ ). Half of the cells were not flagged. For the end user it is not important whether the flagged cells are counted correctly or not, since they all require review. It is, however, important for the assessment of the algorithm.

Num. of spots	Manual count	Program count					
		Not flagged			Flagged (must be reviewed)		
		Agree	Disagree	Total	Agree	Disagree	Total
4	1	 1	0	1	0	0	0
3	60	 29	0	29	 22	 9	31
2	29	 14	0	14	 2	 13	15
1	4	 2	0	2	 2	0	2
<b>Total</b>	94	46	0	46	26	22	48

Distributions of spot counts were analyzed by  $\chi^2$  test<sup>11</sup>. Each line in Fig. 12 has the  $\chi^2$  results between manual and program spot counts. Normally the spot counting is done at the time of probe acquisition, but in the case of this study it was repeated later because the software was not finalized at the time of image acquisition.

Over 28 scans, the average percent of cells not flagged by the program (and therefore not needing operator review) is 49.8%, and correlates with the visual assessment of the quality of the slide. The average percent of agreement between manual and program spot counts for unflagged cells is 97.6% for the 28 scans, and is never less than 90%. In all scans (with the exception of A2307) there is no significant difference between the distributions obtained by manual and program spot counting. In the 12 samples that have two scans, the difference between program spot distributions is bigger in 8 and smaller in 4 than between manual spot distributions.



Sample	Manual count				Program count				chi-sq.	df	p	% not flagged	% agree
	1	2	3	>3	1	2	3	>3					
C3248	4	29	60	1	2	14	29	1	0.27	3	0.97	49	100
CPH898	7	54	6		9	39	1		3.53	2	0.17	73	90
C3021	9	58	0		8	21	0		2.78	2	0.25	43	100
A2307	16	101	11		12	31	1		6.57	2	0.04	34	91
A2307b	31	121	6		9	65	4		2.53	2	0.28	49	97
A2391	10	71	10	9	1	8	0	0	7.15	3	0.07	9	100
A2391b	9	57	13	2	2	6	2	0	1.05	3	0.79	12	90
A2397	7	51	2		4	14	0		1.78	2	0.41	30	100
A2397b	16	37	10		6	6	0		4.12	2	0.13	19	92
A2519	13	68	7	1	6	13	1	0	2.91	3	0.41	22	100
A2519b	15	105	4	1	8	57	1	0	1.03	3	0.79	53	100
A2597	6	56	0		5	40	1		1.42	2	0.49	74	98
A2597b	6	113	7	2	2	19	0	0	2.27	3	0.52	16	100
A2600	9	113	6		3	12	1		2.70	2	0.26	13	94
A2600b	10	106	11	1	6	75	3	1	2.29	3	0.51	66	100
A2604	2	50	4		0	31	1		1.85	2	0.39	57	100
A2604b	18	78	5	0	16	57	4	1	1.57	3	0.67	77	96
A2610	0	50	0		0	42	0		0	2	1.00	84	100
A2610b	7	75	8		3	39	1		2.06	2	0.36	48	100
A2616	3	56	1		3	43	0		0.87	2	0.65	77	100
A2616b	5	59	3		4	42	0		2.14	2	0.34	69	100
A2625	0	62	3	1	1	49	0	0	4.40	3	0.22	76	98
A2625b	7	60	2		3	26	0		0.86	2	0.65	42	100
A2657	2	51	0		1	32	0		0.03	2	0.99	62	100
A2657b	8	44	1		5	21	0		0.68	2	0.71	49	100
A2662	2	72	2		3	43	0		2.27	2	0.32	61	98
A2662b	12	47	3		6	24	1		0.13	2	0.94	50	100
A2871	4	44	2		4	36	0		1.71	2	0.43	80	90

Fig. 12. Summary results of program and manual spot counts of chromosome 21. Slides from 3 CVS and 13 amniocentesis samples provided by Rigshospital, Copenhagen were analyzed. Twelve of these slides were analyzed in two different areas. The duplicate experiments are shown with a gray background. Agreement between manual and program spot counts is calculated on cells not flagged by the program.

## 6. CONCLUSIONS

1. Probe images acquired as maximum projection of Z-stack with 40X objective and presented as monochrome for each probe filter and as color composites are sufficient, if not superior, for spot counting than images in the microscope.
2. A method for counting probe spots in interphase nuclei was developed and formal rules for cell rejection were formulated and parameterized.
3. The presented automated procedure makes it possible to analyze 2-3 times more cells than is practical by a manual procedure. It creates a permanent record of analysis for later evaluation.
4. By applying stringent cell rejection criteria, the problem of spot counting is converted from a problem of interpretation and disagreement between observers into a problem of throughput.

## 7. ACKNOWLEDGEMENTS

The work was done in collaboration with J. Philip, B. Christiansen, L. Lykke Hansen, and I. Garn from the Chromosome Laboratory, Section of Clinical Genetics, The Rigshospital, University of Copenhagen, Denmark, and J. Hoovers, M. Jakobs, I. De Graaf from the Department of Clinical Genetics, University of Amsterdam, The Netherlands.

## 8. REFERENCES

1. T. Bryndorf, B. Christensen, M. Vad, J. Parner, V. Brocks , and J. Philip, "Prenatal detection of chromosome aneuploidies by fluorescence *in situ* hybridization: experience with 2000 uncultured amniotic fluid samples in a prospective preclinical trial", *Prenatal Diagnosis*, **17**, pp. 333-341, 1997
2. B. Eiben, W. Trawicki, W. Hammans, R. Goebel and J.T. Epplen, "A prospective comparative study on fluorescence *in situ* hybridization (FISH) of uncultured amniocytes and standard karyotype analysis", *Prenatal Diagnosis*, **18**, pp. 901-906, 1998
3. I. Ravkin, V. Temov, "Automated microscopy system for detection and genetic characterization of fetal nucleated red blood cells on slides", Proceedings of SPIE (Optical Investigation of Cells In Vitro and In Vivo), v. 3260, pp. 180-191, 1998.
4. H. Netten, L.J. van Vliet, H. Vrolijk, W.C.R. Sloos, H.J. Tanke, I.T. Young, "Fluorescent dot counting in interphase cell nuclei", *Bioimaging* **4**: pp. 93-106, 1996
5. H. Netten, *Automated Image Analysis of FISH Stained Cell Nuclei*, Delft University Press, Delft, 1997
6. H. Netten, I.T. Young, L.J. van Vliet, H.J. Tanke, H. Vrolijk, W.C.R. Sloos, "FISH and Chips: Automation of fluorescent dot counting in interphase cell nuclei", *Cytometry* **28**: pp. 1-10, 1997
7. C. Ortiz de Solorzano, A. Santos, I. Vallcorba, J.-M. Garcia-Sagredo, and F. del Pozo, "Automated FISH spot counting in interphase nuclei: statistical validation and data correction", *Cytometry*, **31**, pp. 93-99, 1998
8. J. Serra, *Image Analysis and Mathematical Morphology*, Vol. 1. Academic Press, London, 1989
9. S. Beucher and F. Meyer, "The Morphological Approach to Segmentation: The Watershed Transformation" in: *Mathematical Morphology in Image Processing*, E.R. Dougherty – Ed., pp. 433 – 481, Marcel Dekker, New York, 1993
10. G.A. Korn, T.M. Korn, *Mathematical Handbook for Scientists and Engineers*, McGraw-Hill, New York, 1961
11. Statlets, statistical package from NWP Associates, Inc. ([www.statlets.com](http://www.statlets.com))